**substance: $TmSe_{1-x}Te_x$**
**property: crystal structure, physical properties**

**(energy gap $E_g$, lattice parameter $a$, resistivity $\rho$, compressibility $\kappa$, magnetic moment $p_{eff}$, paramagnetic Curie temperature $\Theta_p$, Neel temperature $T_N$)**

| | | | | |
|---|---|---|---|---|
| | | | lattice constant vs. x: Fig. 1, | |
| $E_g$ | 0.3 eV | x = 1 | pressure-volume curve: Fig. 2 | 90N, |
| | 0.04 eV | x = 0.4 | | 85B |
| | | | resistivity vs. x: Fig. 3, Fig. 4 | |
| | | | x ≥ 0.4: semiconductor | |
| x = 0.4 | | | | 85B |
| $a$ | 6.02 Å | | | |
| $E_g$ | 0.040 eV | | | |
| $dE_g/dp$ | –67 meV/GPa | low pressure | | |
| $\rho$ | $1.8 \cdot 10^{-3}$ Ωcm | $p = 10^5$ Pa | semiconductor-metal transition: 0.3 GPa | |
| | $3.2 \cdot 10^{-4}$ Ωcm | $p > 0.3$ GPa | | |
| $\kappa$ | $4.5 \cdot 10^{-11}$ $Pa^{-1}$ | | compressibility | |
| $p_{eff}$ | 4.56 $\mu_B$ | | effective magnetic moment | |
| $\Theta_p$ | –2 K | | paramagnetic Curie temperature | |
| $T_N$ | 0.30 K | | Néel temperature | |
| x = 0.5 | | | | 81B |
| $a$ | 6.07 Å | | | |
| $E_g$ | 0.180±20 eV | | | |
| $dE_g/dp$ | –100±10 meV/GPa | | | |
| $d \log\rho/dp$ | 1.6 decades/GPa | | resistivity vs. $T$: Fig. 5 | |
| | | | magnetic susceptibility vs. $T$: Fig. 6 | |
| | | | magnetic moment: Fig. 7 | |
| $\kappa$ | $2.2 \cdot 10^{-11}$ $Pa^{-1}$ | | compressibility | |
| x = 0.55 | | | | 90N |
| $a$ | 6.137 Å | | neutron scattering and $a$ vs. $T$: Fig.: 8 | |
| $E_g$ | 0.135 eV | | pressure dependence of resistivity: Fig. 9 | |
| | 0.108 eV | | temperature dependence of resistivity: Fig. 10 | |
| $dE_g/dp$ | –118 meV/GPa | | | |
| | | | pressure and temperature dependence | |
| | | | of resistivity: Fig. 11 | |
| | | | magnetoresistance: Fig. 12 | |
| | | | magnetic susceptibility vs. $T$: Fig. 13 | |
| | | | imaginary part of the dielectric function | |
| | | | and Raman scattering: Fig. 14 and 15 | |
| $a$ | 6.14 Å | | | 85B |
| $E_g$ | 0.110 eV | | | |
| $dE_g/dp$ | –126 meV/GPa | low pressure | | |
| | –99 meV/GPa | high pressure | | |
| $\rho$ | $3.2 \cdot 10^{-2}$ Ωcm | $p = 10^5$ Pa | semiconductor-metal transition: 1.2 GPa | |
| | $4.0 \cdot 10^{-4}$ Ωcm | $p > 1.2$ GPa | | |
| $\kappa$ | $3.3 \cdot 10^{-11}$ $Pa^{-1}$ | $p = 10^5$ Pa | compressibility | |
| | $35 \cdot 10^{-11}$ $Pa^{-1}$ | $p = 1.2$ GPa | | |
| $p_{eff}$ | 4.51 $\mu_B$ | | effective magnetic moment | |
| $\Theta_p$ | –2 K | | paramagn. Curie temperature | |
| x = 0.68 | | | | 90N |
| $a$ | 6.21 Å | | | |
| $E_g$ | 0.185 eV | | | |
| | 0.156 eV | | | |
| $dE_g/dp$ | –130 meV/GPa | | | |
| | | | pressure dependence of resistivity: Fig: 16 | |
| | | | temperature dependence of resistivity: Fig. 17 | |

| | | | | |
|---|---|---|---|---|
| $a$ | 6.21 Å | | | 85B |
| $E_g$ | 0.170 eV | | | |
| $dE_g/dp$ | –130 meV/GPa | low pressure | | |
| | –110 meV/GPa | high pressure | | |
| $\rho$ | 0.28 Ωcm | $p = 10^5$ Pa | semiconductor-metal transition: 1.4 GPa, | |
| | $3.6 \cdot 10^{-4}$ Ωcm | $p > 1.4$ GPa | resistivity and electron concentration vs. pressure: Fig. 18 | |
| $\kappa$ | $3.0 \cdot 10^{-11}$ $Pa^{-1}$ | $p = 10^5$ Pa | compressibility; | |
| | $17 \cdot 10^{-11}$ $Pa^{-1}$ | $p = 1.4$ GPa | bulk modulus, volume vs. pressure: Fig. 19 | |
| $p_{eff}$ | 4.61 $\mu_B$ | | effective magnetic moment | |
| $\Theta_p$ | –2 K | | paramagn. Curie temperature | |
| $T_N$ | 0.20 K | | Néel temperature | |
| x = 0.77 | | | | 81B |
| $a$ | 6.245 Å | | | |
| $E_g$ | 0.240±30 eV | | | |
| $dE_g/dp$ | –110±10 meV/GPa | | | |
| $d \log\rho/dp$ | 1.8 decades/GPa | | | |
| $\kappa$ | $(2.3 \pm 0.1) \cdot 10^{-11}$ $Pa^{-1}$ | | compressibility | |
| x = 0.83 | | | | 81B |
| $a$ | 6.28 Å | | | |
| $E_g$ | 0.250 ± 30 eV | | | |
| $dE_g/dp$ | –125±10 meV/GPa | | | |
| $d \log\rho/dp$ | 2.1 decades/GPa | | | |
| $\kappa$ | $(2.4 \pm 0.05) \cdot 10^{-11}$ $Pa^{-1}$ | | compressibility | |
| $a$ | 6.28 Å | | | 85B |
| $E_g$ | 0.210 eV | | | |
| $dE_g/dp$ | –140 meV/GPa | low pressure | | |
| | –98 meV/GPa | high pressure | | |
| $\rho$ | 1.5 Ωcm | $p = 10^5$ Pa | semiconductor-metal transition: 2.0 GPa | |
| | $4.0 \cdot 10^{-4}$ Ωcm | $p > 2.0$ GPa | | |
| $\kappa$ | $2.4 \cdot 10^{-11}$ $Pa^{-1}$ | $p = 10^5$ Pa | compressibility | |
| | $9 \cdot 10^{-11}$ $Pa^{-1}$ | $p = 1.9$ GPa | | |
| x = 1 | | | | 81B |
| $a$ | 6.34 Å | | | |
| $E_g$ | 0.320±40 eV | | | |
| $dE_g/dp$ | –100±10 meV/GPa | | | |
| $\kappa$ | $2.65 \cdot 10^{-11}$ $Pa^{-1}$ | | compressibility | |
| $a$ | 6.36 Å | | | 85B |
| $E_g$ | 0.300 eV | | | |
| $dE_g/dp$ | –110 meV/GPa | low pressure | | |
| $\rho$ | 18 Ωcm | $p = 10^5$ Pa | semiconductor-metal transition: 2.5 GPa | |
| $\kappa$ | $2.2 \cdot 10^{-11}$ $Pa^{-1}$ | $p = 10^5$ Pa | compressibility | |
| $p_{eff}$ | 4.73 $\mu_B$ | | effective magnetic moment | |
| $\Theta_p$ | –1.5 K | | paramagn. Curie temperature | |
| $T_N$ | 0.235 K | | Néel temperature | |

## References:


81B Batlogg, B.: Phys. Rev. B 23(2) (1981) 650.
85B Boppart, H.: J. Magn. Magn. Mater. 47/48 (1985) 436.
90N Neuenschwander, J., Wachter, P.: Physica B 160 (1990) 231.

**Fig. 1**.

$TmSe_{1-x}Te_x$. Lattice parameter as a function of the stoichiometry x [85B]. Straight lines: Vegard-law for given valences.

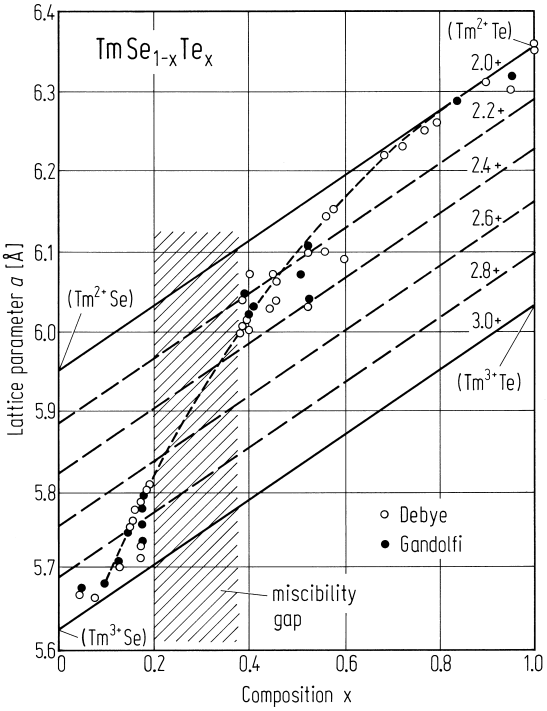

**Fig. 2**.

$TmSe_{1-x}Te_x$. Pressure-volume diagram at 300 K [85B]. The dashed curve indicates the deviation from the Vegard-law line for divalent Tm.

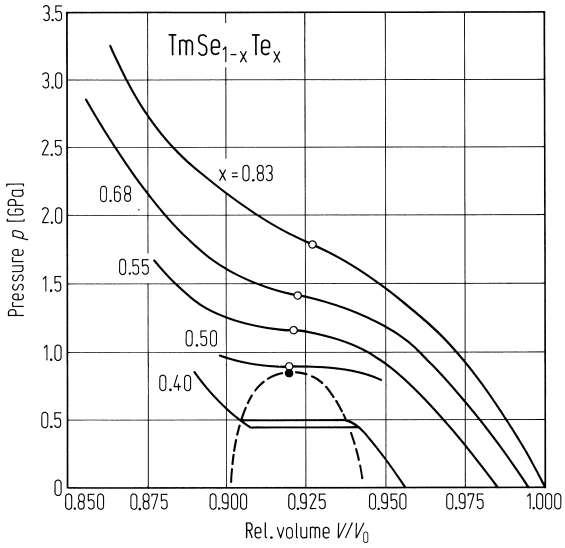

**Fig. 3**.

$TmSe_{1-x}Te_x$. Pressure dependence of the resistivity at various stoichiometries x at 300 K [85B].

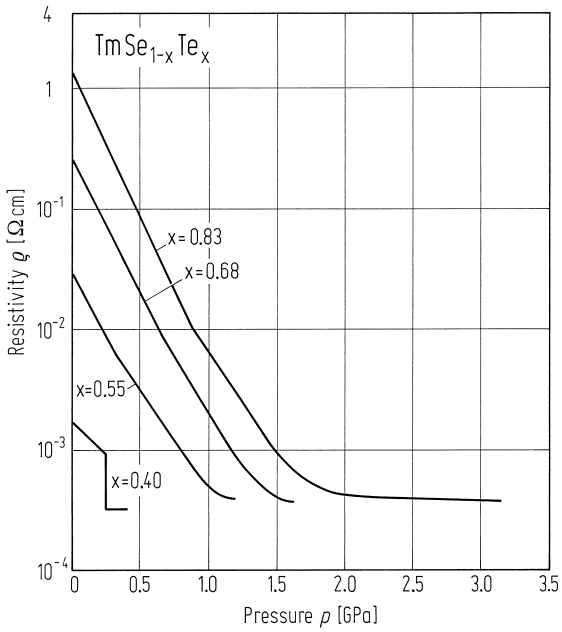

**Fig. 4**.

$TmSe_{1-x}Te_x$. Electrical resistivity at ambient temperature and pressure [81B].

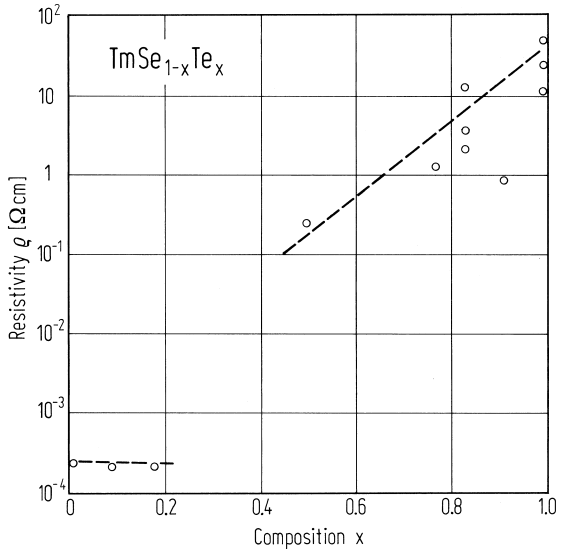

**Fig. 5**.

$TmSe_{1-x}Te_x$. Arrhenius plot of the electrical resistivity of semiconducting $TmSe_{1-x}Te_x$ (x = 0.5 and 0.83) [81B]. Inset shows high *T* behavior on an expanded scale for x = 0.83.

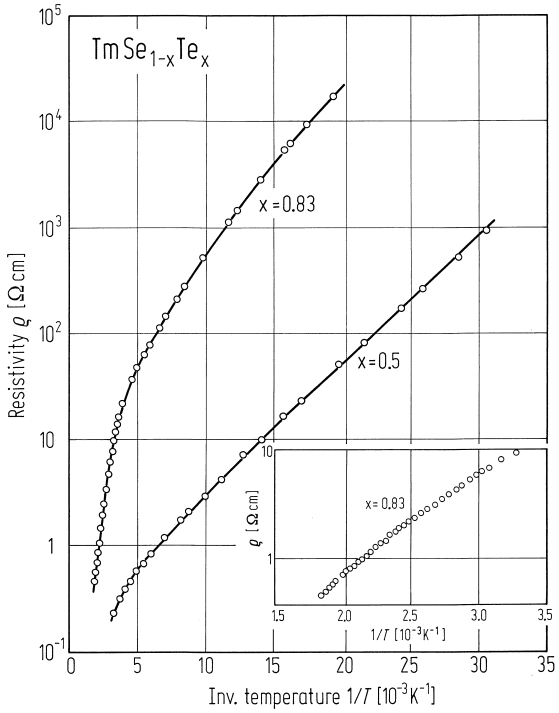

**Fig. 6**.

$TmSe_{0.5}Te_{0.5}$. Inverse magnetic susceptibility (in CGS-emu) as a function of temperature [81B]. Inset shows low *T* behaviour on an expanded scale.

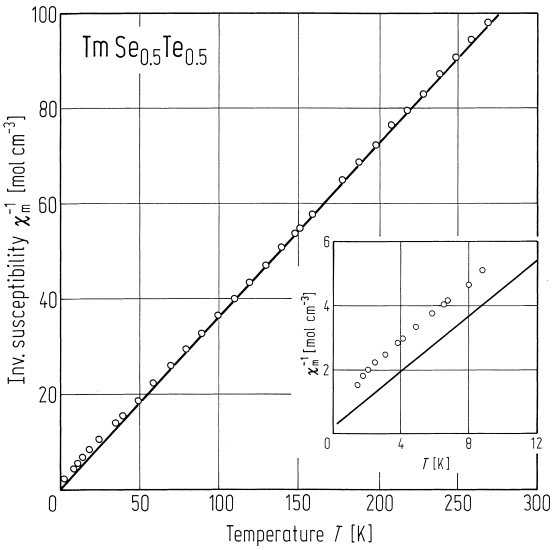

**Fig. 7**.

$TmSe_{0.5}Te_{0.5}$. Magnetic moment per formula unit $p_{FU}$ vs. magnetic field at $T$ = 4.2 K [81B].

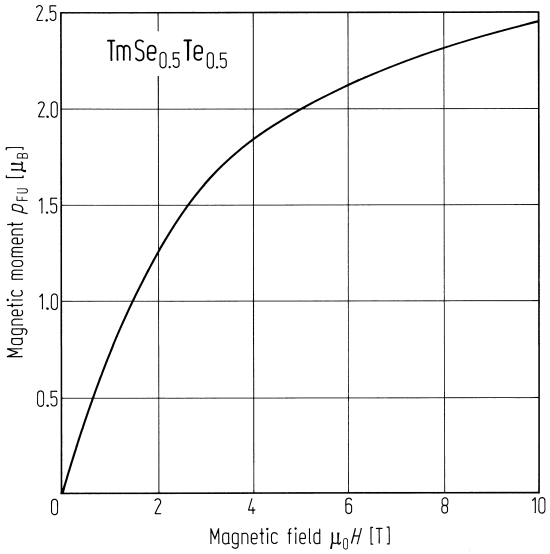

**Fig. 8**.

$TmSe_{0.45}Te_{0.55}$. Neutron scattering at $p$(300 K) = 1.19 GPa. **(a)** Temperature dependence of the peak width of the nuclear Bragg reflections 200 and 400 in a 2:1 scan. The horizontal lines are guides to the eye. **(b)** Temperature dependence of the lattice parameter $a$. Below 255 K $a$ increases by 1.6% indicating the valence transition [90N].

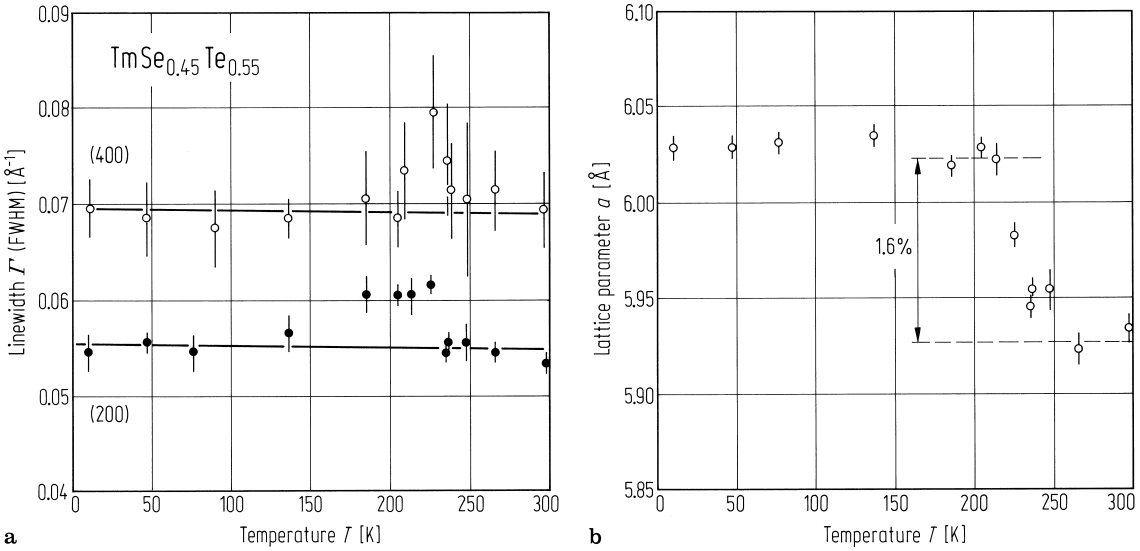

**Fig. 9**.

$TmSe_{0.45}Te_{0.55}$. Pressure dependence of the electrical resistivity for various temperatures. The thin solid lines are guides to the eye. For temperatures below 200 K a first order SMT is suggested [90N].

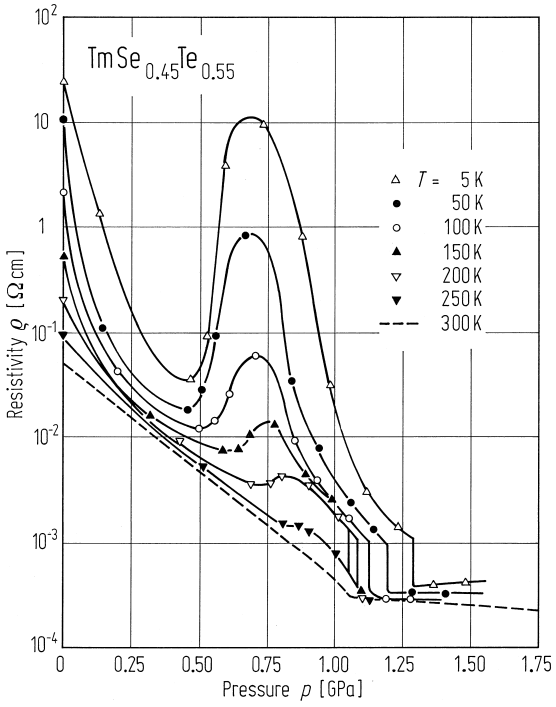

**Fig. 10**.

$TmSe_{0.45}Te_{0.55}$. Temperature dependence of the electrical resistivity. The pressures at room temperature are *a*: 0, *b*: 0.97, *c*: 1.10, *d*: 1.29, *e*: 1.50 and *f*: 1.70 GPa, respectively. Note the linear scale for the resistivity in the insert. For clarity not all measured curves are shown [90N].

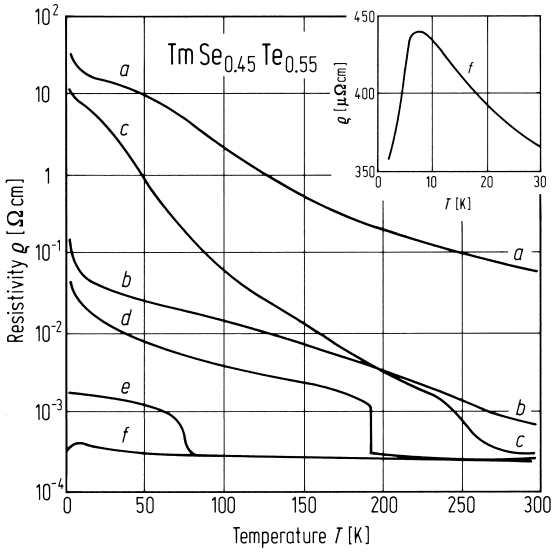

**Fig. 11**.

$TmSe_{0.45}Te_{0.55}$. Temperature dependence of the electrical resistivity for three different pressure runs. At room temperature the pressure is 1.20, 1.29 and 1.39 GPa and at the transition it is reduced to 1.07, 1.10 and 1.10 GPa, respectively [90N].

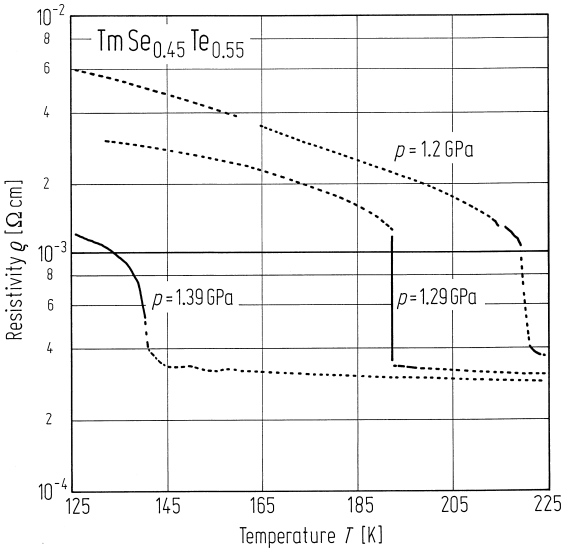

**Fig. 12**.

$TmSe_{0.45}Te_{0.55}$. Magnetoresistivity $\Delta\rho_0/\rho_0$ as a function of magnetic field at various pressures and temperatures. At 0.75 and 1.28 GPa the sample is in the semiconducting phase, at 1.52 GPa it is metallic [90N].

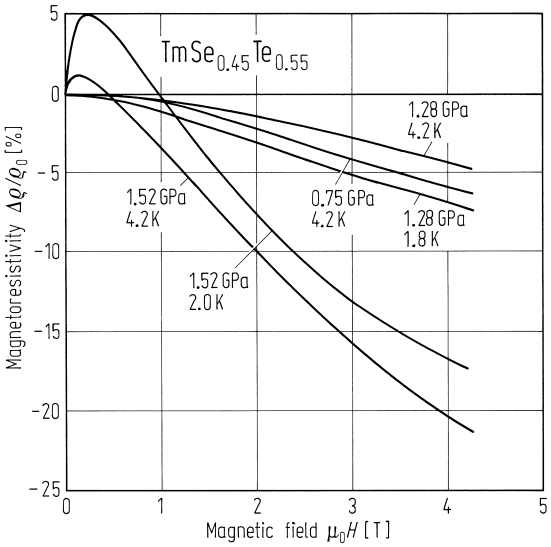

**Fig. 13**.

$TmSe_{0.45}Te_{0.55}$. Induced voltage (magnetic susceptibility) as a function of temperature for various pressures, whose magnitudes are indicated for $T$ = 5 K. In the metallic state ($p$ = 1.43 and 1.64 GPa) a pronounced peak structure can be observed, whereas in the semiconducting state ($p$ = 0.85 and 1.36 GPa) the susceptibility remains very small [90N].

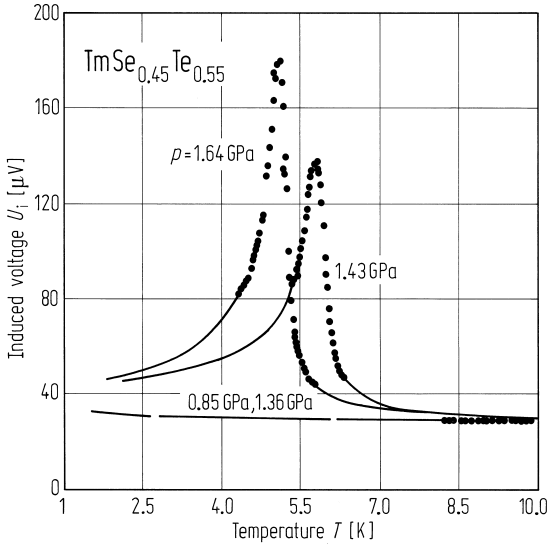

**Fig. 14**.

$TmSe_{0.45}Te_{0.55}$. Imaginary part ($\varepsilon_2$) of the dielectric function at $p = 0$ as a function of the photon energy. Solid line: $T = 6$ K, dashed line $T = 300$ K. In the insert $\varepsilon_2$ is magnified in the energy range $10^{-2}$...100 eV; the structure at 60meV (arrow) is suggested to be due to an exciton [90N].

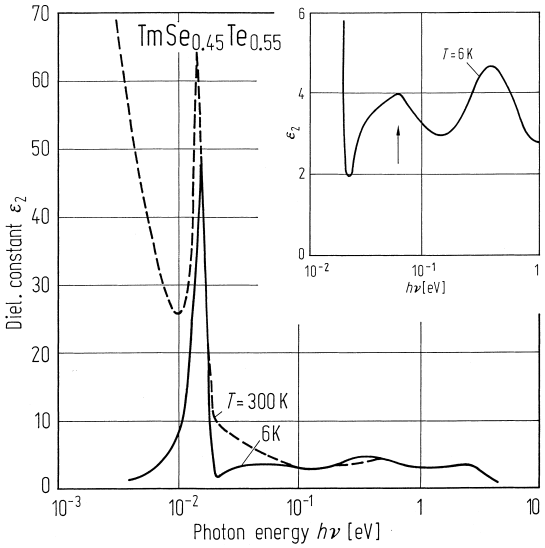

**Fig. 15**.

$TmSe_{0.45}Te_{0.55}$. Raman scattering at $p = 0$ and $T = 50$ K [90N].

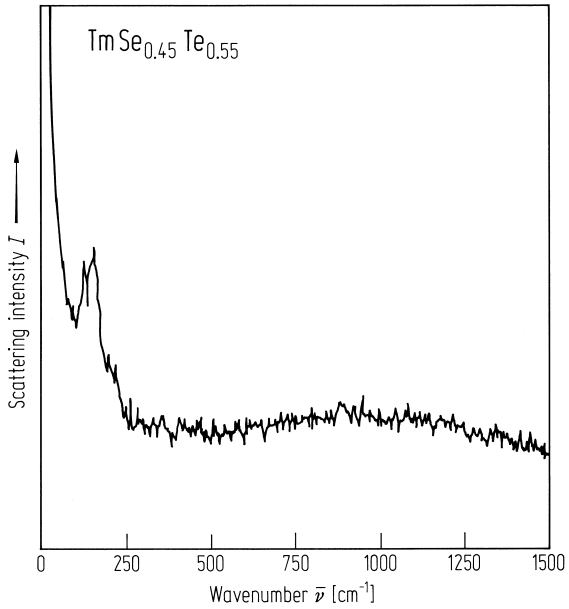

**Fig. 16**.

$TmSe_{0.32}Te_{0.68}$. Pressure dependence of the electrical resistivity for various temperatures. The solid lines are guides to the eye [90N].

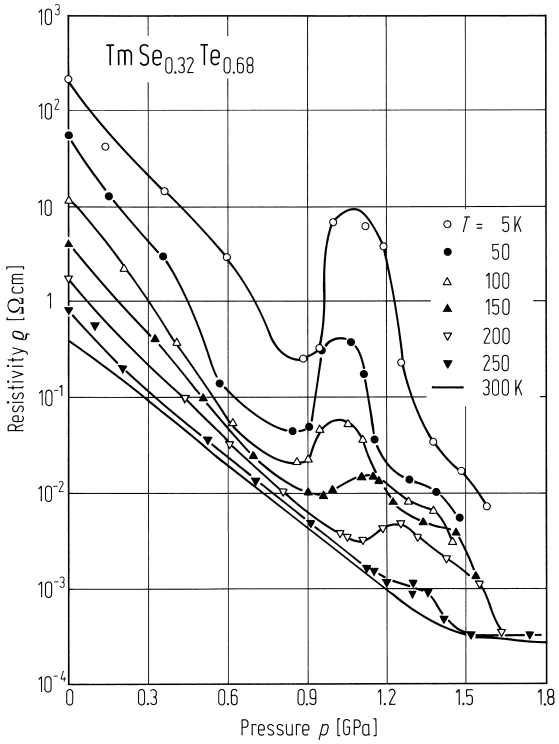

**Fig. 17**.

$TmSe_{0.32}Te_{0.68}$. Temperature dependence of the electrical resistivity. The pressures at room temperature are between 0 and 1.8 GPa. For clarity not all measured curves are shown [90N].

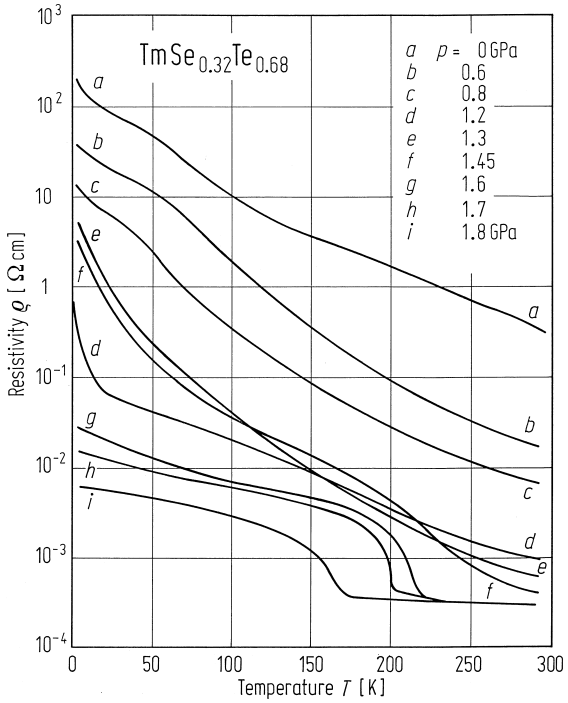

**Fig. 18**.

$TmSe_{0.32}Te_{0.68}$. Pressure dependence of the electrical resistivity and electron concentration at 300 K [85B].

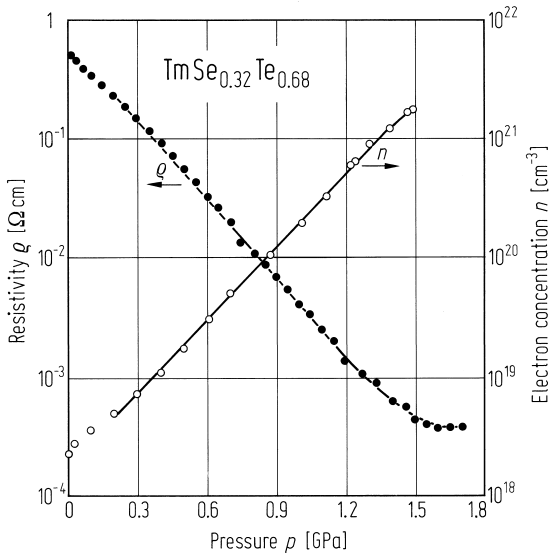

## Fig. 19.

$TmSe_{0.32}Te_{0.68}$. Pressure dependence of the volume and the bulk modulus at 300 K [85B]. The dashed line in **(a)** represent the theoretical variations of a pure divalent and trivalent compound, the dotted line is calculated from Hall effect data. The dashed line in **(b)** is calculated from elastic constants $c_{11}$ and $c_{12}$.